

GALACTIC DUST PROPERTIES

D. Paradis^{1,2} and the Hi-GAL team

Abstract. Recent studies have shown evidence for variations in the dust emissivity law with temperature and wavelength. A recent dust emission model, called TLS model (for two-level systems), based on the description of the disordered internal structure of the amorphous dust grains has been developed to interpret observations in the far-infrared/submillimeter (FIR/submm) domain. A recent work focusing on the comparison between data of the diffuse interstellar medium seen by FIRAS-WMAP, as well as Archeops compact sources, with the TLS model allowed us to constrain the model parameters characterizing the general Galactic dust properties. Using the newly available Herschel/Hi-GAL data of the inner Galactic plane, we report a 500 μm emissivity excess in the peripheral parts of the Galactic plane, that can reach up to 20% of the emissivity. Results of the TLS modeling indicate significant changes in the dust properties from the central to peripheral parts of the Galactic plane.

Keywords: dust, extinction, infrared, ISM

1 Introduction

The study of the extended far-infrared (FIR) and submillimeter (submm) sky emission is a relatively young subject. This wavelength range is dominated by emission from large silicate-based interstellar grains, that dominate the total dust mass and radiate at thermal equilibrium with the surrounding radiation field. Their emission is often modeled using a modified black body at a given dust temperature and a fixed spectral index (β). The FIR/submm emission is routinely used to infer total gas column density and mass of objects ranging from molecular clouds to entire external galaxies, assuming that dust faithfully traces the gas. The data analysis of balloon (PRONAOS, Archeops) and satellite (FIRAS, WMAP) data has revealed that the FIR/submm emission cannot be explained by a simple extrapolation of the mid-IR emission:

- Dust emissivity appears to be wavelength-dependent with the emission spectrum flattening in the submm as compared to a modified black-body emission (Reach et al. 1995; Finkbeiner et al. 1999; Galliano et al. 2005; Paladini et al. 2007).
- Dust emissivity appears to be temperature-dependent, the emissivity spectra being flatter with the increasing dust temperature (Dupac et al. 2003; Désert et al. 2008).

Similar variations are now seen in laboratory spectroscopic experiments on amorphous dust analogs (Agladze et al. 1996; Mennella et al. 1998; Boudet et al. 2005). In particular, recent studies on three analogs of amorphous silicate Mg_2SiO_4 , MgSiO_3 , and $\text{CaMgSi}_2\text{O}_6$ reveal that this temperature and wavelength dependence of the absorption is observed on all the samples, but disappear when the same samples are annealed until crystallization (Coupeaud et al. 2011).

These analyses indicate that the T_d - β variations are likely to result from intrinsic dust properties that can be reproduced for the first time by a dust emission model such as the two-level systems (TLS) one.

Dust emissivity also appear to be environment-dependent, with an absolute emissivity value in the far-IR increased in cold and dense environments, as seen in the Taurus cloud (Stepnik et al. 2003; Planck Collaboration 2011a).

¹ Université de Toulouse; UPS-OMP, IRAP, Toulouse, France

² CNRS; IRAP, 9 av. du Colonel Roche, BP 44346, 31028, Toulouse, cedex 4, France

2 Evolution of dust properties from diffuse to dense medium

We analyze the dust emission from the outer Galactic plane using DIRBE, Archeops and WMAP data from 100 μm to 3.2 mm. We perform a correlation study of the FIR-mm emission with gas tracers in individual regions, and derive the average equilibrium temperature of large dust grains in both molecular and atomic phases in a set of regions along the Galactic plane. We use this temperature to derive the emissivity spectra for each phase and region.

We show that the emissivity spectra are always steeper in the FIR ($\lambda < 600 \mu\text{m}$) and flatten in the submm and mm. In regions where dust is significantly colder in the molecular phase than in the surrounding atomic medium, we produce an increase in the emissivity by a factor of $\simeq 3$ in the FIR (see Fig. 1, panel A). However, we showed that the emissivity increase is restricted to the FIR range; the emissivity spectra for the dust in the atomic and molecular phases become comparable again in the submm and mm wavelength range.

We interpret the FIR emissivity excess in the molecular clouds containing cold dust as being caused by the coagulation of large grains into fractal aggregates. The fact that the emissivities do reconcile in the submm could be related to the amorphous nature of the grains contained in the aggregates (see the following Section).

The full description of this analysis is presented in Paradis et al. (2009).

3 A model of amorphous dust: the TLS model

The recent TLS model (Mény et al. 2007) is based on the solid-state physics model developed to interpret specific properties of the amorphous solids identified in laboratory data. As a consequence, it is expected to apply with a high degree of universality, and not to be sensitive to the exact chemical nature of the dust. The disordered charge distribution (DCD) part of the model describes the interaction between the electromagnetic wave and acoustic oscillations in the disordered charge of the amorphous material (Vinogradov, 1960; Schlomann, 1964). This charge-disorder is observed on nanometer scale and is described here by a single charge correlation length. The TLS part models the disorder at atomic scale by a distribution of asymmetric double-well potential (ADWP). Each ADWP can be viewed as to close configurations of atoms or group of atoms in the disordered structure (Phillips 1972, 1987; Anderson et al. 1972). The TLS model describes the interaction of the electromagnetic wave with a simple distribution of two-level systems that represent the lowest states (ground states) of the ADWP. Both DCD and TLS phenomena have been first applied by Bösch (1978) to explain the observed temperature dependence of the absorption of some silica-based glasses in the FIR/mm. Three interaction mechanisms, which all depend on temperature, can occur in such a population of TLS sites: a resonant absorption, and two relaxation processes identified as “tunneling relaxation” and “hopping relaxation”.

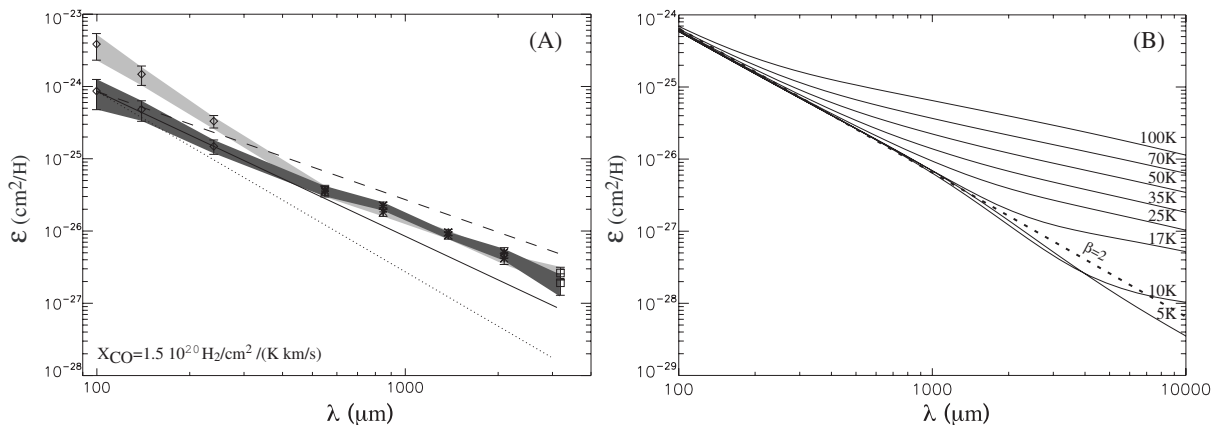


Fig. 1. Left: Panel (A): Median dust emissivity SEDs for regions with dust significantly colder in the molecular phase than in the surrounding atomic medium. The molecular emissivity has been scaled to match that of the atomic phase in the range 550 μm –3 mm. The DIRBE, Archeops and WMAP data correspond to diamond, star and square symbols, respectively. The shaded areas show the $\pm 1\text{-}\sigma$ dispersion around each emissivity SED, in dark and light grey for the atomic and molecular phase. For comparison, power-law spectra with $\beta=1.5$ (dashed), $\beta=2$ (solid) and $\beta=2.5$ (dot) are shown, normalized to the atomic emissivity at 100 μm . **Right:** Panel (B): Predicted emissivity with the TLS model, as a function of wavelength for different temperatures. The dashed line shows a λ^{-2} emissivity power-law.

The TLS model is compared to astrophysical data, such as the FIRAS/WMAP and Archeops data. The FIRAS/WMAP spectrum represents the diffuse interstellar medium in the stellar neighborhood, whereas the Archeops data characterize dust properties in a variety of compact sources, where a significant inverse relationship between the dust temperature and the emissivity spectral index had been shown. We performed a χ^2 minimization to determine standard values for the parameters of the TLS model selected to capture the spectral and temperature variations in the model. These free parameters are the dust temperature (T_{TLS}), the charge correlation length (l_c) that controls the wavelength where the inflection point between the two $\beta = 2$ and $\beta = 4$ ranges occurs, the intensity factor of the TLS processes (A) with respect to the DCD effect, and the intensity factor of the TLS/hopping process (c_Δ). Results indicate that emission in the submm/mm is dominated by the hopping relaxation. According to the model, the BG emission in the FIR/mm domain depends on wavelength and temperature, which is fundamental both for dust mass determination from FIR/submm measurements but also for component separation. Using the best-fit parameters ($T_{TLS} = 17.26$ K, $l_c = 13.4$ nm, $A = 5.81$, and $c_\Delta = 475$) allowing reproduction of both the emission from the diffuse medium and the compact sources, the model predicts significant β variations for temperatures between 5 and 100 K, with a maximum value of 2.6 at 2 mm. The TLS model is presently the only astrophysical model able to predict β variations with temperature and wavelengths, as observed in both observational and laboratory data. The dust emissivity can be seriously underestimated if its variations with temperature and wavelength are not taken properly into account (see Fig. 1, panel B), generally inducing overestimates of the dust mass. We also predict dust emissivities in the IRAS 100 μm , Herschel, and Planck bands for temperatures between 5 and 100 K, which are useful for comparison with the Planck and Herschel data.

The full description of this analysis is presented in Paradis et al. (2011a).

4 Dust properties along the Galactic plane using Hi-GAL data

We investigate variations in the spectral index of the dust emissivity, with temperature and wavelength, in the inner Galactic plane, using Herschel observations in two Hi-GAL ($160 \mu\text{m} < \lambda < 500 \mu\text{m}$) fields, centered at $l = 30^\circ$ and $l = 59^\circ$, acquired during the Herschel Science Demonstration phase, combined with the IRIS 100 μm data, $4'$ angular resolution. We fit the spectral energy distribution (SEDs) for each pixel of the two fields with two independent methods (least-square fit and maximum likelihood using a Monte Carlo Markov Chain algorithm, hereafter MCMC), deriving simultaneously the emissivity spectral index and the dust temperature by adjusting a modified blackbody function to the data. The results are similar with both methods. Using the MCMC method we computed the 68% likelihood contours for each point. We find a T_d - β inverse correlation, with the local variation going from 1.8 to 2.6 for temperatures between 14 and 23 K, shown for the first time in the inner Galactic plane. The median value of β is similar in both fields, equal to 2.3, slightly higher than the usual reference value of 2.

With the newly released Hi-GAL data combined with the IRIS 100 μm data, we perform an analysis of the emissivity variations along the Galactic plane. Changes in the emissivity spectra are interpreted in terms of the TLS model (see Fig. 2). We report:

- A 500 μm emissivity excess with respect to the predictions of a modified black-body model with $\beta=2$, in the peripheral parts of the Galactic plane ($35^\circ < |l| < 70^\circ$) covered by the data. This excess can represent up to 16% to 20% of the total emission. A similar excess has recently been evidenced in the Large Magellanic Cloud (Gordon et al. 2010; Galliano et al. 2011)
- Warmer dust temperatures in the central ($|l| > 35^\circ$) than in the peripheral Galactic regions.
- A flattening of the emissivity spectra in the range 100-500 μm with increasing dust temperature, that does not result from temperature mixture along the line of sight.
- The 500 μm emissivity excess can be explained by an increase in the intensity of the TLS processes, indicating a larger degree of amorphization of the grains in the peripheral parts of the Galactic plane.
- Dust properties along the Galactic plane seem to be different from those of the solar neighborhood, the excess being smaller in the latter than expected from an extrapolation of the Galactic plane behavior.

The full description of this analysis is presented in Paradis et al. (2011b).

5 Conclusions

Understanding emission of the big grains dust component is not easy since it varies with wavelength, temperature and environment. We evidenced variations in the emissivity from diffuse to dense medium, from the solar

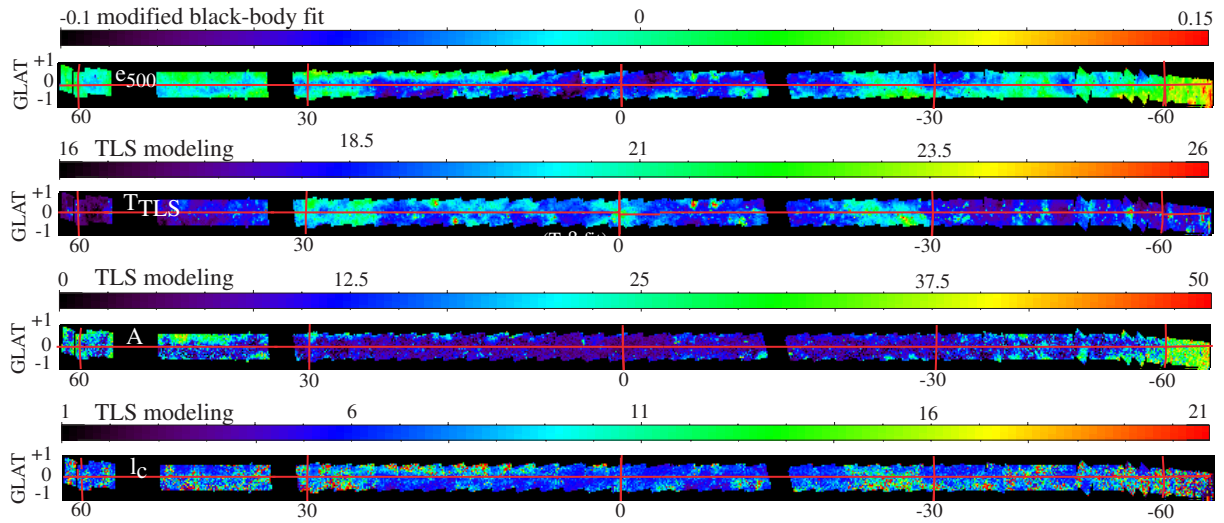


Fig. 2. From top to bottom: 500 μm emissivity excess (e_{500}), and results of the TLS modeling: dust temperature (T_{TLS}) in K, intensity of the TLS processes (A), correlation length (l_c) in nm.

neighborhood to the Galactic plane, and from the central to the peripheral parts of the inner Galactic plane. The presence of submm excess reveals some variations in the optical properties of the interstellar grains. Comparison between astrophysical observations/laboratory data and TLS modeling can lead to deduce more informations on the amorphous state of the grain itself.

References

- Agladze, N. I., Sievers, A. J., Jones, S. A., et al. 1996, *ApJ*, 462, 1026
 Anderson, P. W., Halperin, B. I., & Varma, C. M. 1972, *Phil. Mag.*, 25, 1
 Bösch, M. 1978, *Physical Review Letters*, 40, 879
 Boudet, N., Mutschke, H., Nayral, C., et al. 2005, *ApJ*, 633, 272
 Coupeaud, A., et al. 2011, *A&A*, accepted, arXiv1109.2758
 Désert, F.-X., Macías-Pérez, J. F., Mayet, F., et al. 2008, *A&A*, 481, 411
 Dupac, X., Boudet, N., Giard, M., et al. 2003, *A&A*, 404, L11
 Finkbeiner, D. P., Davis M., Schlegel D.J. 1999, *ApJ*, 524, 867
 Galliano, F., Madden, S. C., Jones, A. P., et al. 2005, *A&A*, 434, 867
 Galliano, F., et al. 2011, *A&A*, accepted
 Gordon, K., et al. 2010, *A&A*, 518, 89
 Mennella, V., Brucato, J. R., Colangeli, L., et al. 1998, *ApJ*, 496, 1058
 Mény, C., et al. 2007, *A&A*, 468, 171
 Paladini, R., et al. 2007, *A&A*, 465, 839
 Paradis, D., Bernard, J.-P., & Mény, C. 2009, *A&A*, 506, 745
 Paradis, D., et al. 2010, *A&A*, 520, 8
 Paradis, D., Bernard, J.-P., Mény, C., & Gromov, V. 2011a, *A&A*, in press, arXiv1107.5179
 Paradis, D., et al. 2011b, *A&A*, submitted
 Phillips, W. 1972, *J. Low Temp. Phys.*, 11, 757
 Phillips, W. 1987, *Rep. Prog. Phys.*, 50, 1657
 Planck Collaboration 2011a, *Planck early results 25*, *A&A*, accepted, arXiv1101.2037
 Reach, W. T., et al. 1995, *ApJ*, 451, 188
 Stepnik, B., Abergel, A., Bernard, J.-Ph., et al. 2003, *A&A*, 398, 551